10th World Congress on Structural and Multidisciplinary Optimization
May 19 -24, 2013, Orlando, Florida, USA

High-order Finite Elements for Topology Optimization

Tam H. Nguyen[1], Chau H. Le[2], Jerome F. Hajjar[3]

[1,3] Northeastern University, Boston, Massachusetts, USA,
th.nguyen@neu.edu, jf.hajjar@neu.edu
[2] Institute of Mechanics and Environmental Engineering, Hanoi, Vietnam
lhchau@imee.vn

1. Abstract
The h-version finite element method (h-version FEM) has been predominantly used in topology optimization to date since it is more suitable for traditional element-based topology optimization strategies. However, the p-version finite element method (p-version FEM) has gained increasing popularity for analysis especially among front-end CAE packages where topology optimization is also used increasingly. In this work, we investigate the use of p-version FEM for topology optimization, and propose a topology optimization method that can take the advantage of the p-version FEM. Unlike the traditional element-based topology optimization method where a density design variable is assigned to each finite element, our approach separates density variables and finite elements so that the resolution of the density field, which defines the structure, can be higher than the finite element mesh. Thus, we can take full advantage of the higher accuracy that p-elements offer and overcome the disadvantage of coarse meshes usually used with p-version FEM. We demonstrate through examples that, with suitable techniques, topology optimization using p-version FEM enables achieving high resolution results with reasonable computational cost.
2. Keywords: p-version FEM, multi-resolution, topology optimization, density method

3. Introduction
Structural topology optimization aims to find an optimal material distribution in a design domain under given boundary conditions. There have been significant advances in topology optimization in the past decades, and topology optimization has emerged as a powerful tool for generating innovative designs in various engineering fields [1]. In the popular element-based density method [2, 3], the design domain is discretized into finite elements, each of which is assigned a design variable (e.g., density) that is optimized. The optimization process results in different values for the design variables that define the optimal structure similar to the way pixels define a gray-scale image. To obtain a more well-defined design, a finer discretization is needed, requiring more computational power. Despite the rapid increase in computer performance, the need for efficient approaches to obtain high-fidelity designs remains, especially for three-dimensional applications.
Numerous efforts to reduce the computational cost of topology optimization have been documented in the literature. One approach is to use parallel computing to expedite the associated finite element analysis (FEA) [4]. Others use fast iterative solvers and nested solution approaches [5, 6], approximate reanalysis [7], and adaptive mesh refinement strategies [8, 9]. There have also been efforts to employ graphics processing units (GPU) [10] to overcome the computational expense challenge. All the above mentioned studies use a traditional element-based topology optimization approach where the same discretization is used for both the finite element mesh and the design variable set. In other recent studies, methods for improving topology optimization resolution by separating the design and the analysis models in a multi-resolution framework have been proposed [11] and demonstrated in large-scale applications including reliability-based optimization [12, 13], geometrical design of thermoelectric generator [14], biomechanics problems [15], interactive topology optimization apps on hand held device [16], and piezocomposite energy harvesting devices [17].
Additionally, various analysis methods have been investigated for topology optimization, among them are meshless method [18, 19], the boundary element method [20, 21], the finite volume method [22], and the isogeometric method [23]. However, the finite element method (FEM) has been most preferred so far. Traditionally, each finite element is assumed to have a constant material density that is represented by a design variable, resulting in the so-called element-based density method. To increase the analysis quality as well as the topology optimization result fidelity, one then refines the finite element mesh, i.e. using h-refinement or the h-version FEM. The h-version FEM is so well suited for the element-based approach topology optimization approach that the two are often thought of as an integral method. As a result, the majority of studies in topology optimization employ the h-version FEM for the analysis. However, the p-version of the finite element method has its own advantages in analysis and is becoming more and more popular especially in front-end design tools such as Creo [24] and ANSYS [25]. In contrast to the h-version FEM, the p-version FEM keeps the finite element mesh

unchanged while increasing the polynomial order of shape functions in order to achieve higher analysis accuracy. With the p-version FEM, the traditional way of assigning a density to each finite element is not an effective approach since refinement of the analyses does not result in improved resolution for the topology. As the polynomial order increases, the resolution of topology optimization does not change to take advantage of the higher analysis accuracy.

There have been some efforts to use high-order elements for topology optimization reported in the literature. Higher-order elements have been used as a means to alleviate the checkerboard problem [26], which is caused by the fact that the analysis using first-order elements within an h-version FEM approach is not accurate enough for the geometry description using an associated element-based topology optimization approach. To avoid the checkerboard problem, second-order elements for analysis can be used. However, in practice, it is more computationally efficient to use a filter [27-29] together with first-order elements to avoid the checkerboard problem. In contrast, the p-version FEM has advantages in analysis and has gained widespread use. Recent efforts have been made to perform topology optimization with higher-order elements [30] where separate material and displacement discretization [11] for topology optimization have been used with the so-called "finite cell method" [30] for analysis. Even though a rather simple heuristic update scheme was used for optimization, promising results were shown. In this paper, the p-version FEM for topology optimization with standard mathematical programming algorithms is proposed. The proposed multi-resolution method allows flexible resolution for topology optimization and takes full advantage of the p-version FEM. The key features of the multi-resolution topology optimization approach using the p-version FEM are demonstrated via numerical examples.

4. The p-version finite element method

The p-version of the finite element method is well developed and documented, e.g. in [31]. This section provides a summary of key aspects relevant to the proposed topology optimization method for the completeness of the paper. The p-version FEM reduces approximation error inherent in finite element approaches by progressively increasing the polynomial degree of element shape functions. An important difference of the p-version FEM from the classical h-version FEM is in the use of hierarchical shape functions that have orthogonality properties. With standard higher-order finite elements, the shape functions are constructed from Lagrange polynomials [32], while the shape functions for the p-version FEM are constructed using Legendre polynomials, which form a hierarchical set. The procedure to construct the stiffness matrix and the load vector from the shape functions is similar to the standard finite element method [31, 32].

Shape functions in two-dimensional space are constructed based on the one-dimensional hierarchical shape functions. The shape functions for quadrilateral elements are presented here, and other two-dimensional elements, such as triangular elements, can be found in [31]. Consider a standard quadrilateral element, denoted as $\Omega_{st}^{q}=[(-1,1)\times(-1,1)]$ and shown in Figure 1. The shape functions of quadrilateral elements are classified into nodal, edge and internal shape functions. The nodal shape functions are the same as shape functions of the standard FEM.

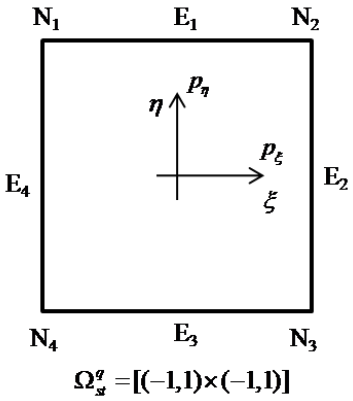

Figure 1. Reference element in standard space with nodes, edges, faces, and polynomial degrees

$$N_{1,1}^{N_i}(\xi,\eta)=\frac{1}{4}(1+\xi_i\xi)(1+\eta_i\eta),\ \ i=1,...,4 \tag{1}$$

Where (ξ_i,η_i) are the coordinates of the i-th node of the reference element. These nodal shape functions are similar to the standard bilinear shape functions for isoparametric quadrilateral element. The edge shape functions differ

from the conventional FEM. For example, the edge shape function for edge E_1 in Figure 1 is defined as follows:

$$N_{i,1}^{E_1}(\xi,\eta)=\frac{1}{2}(1+\eta)\phi_i(\xi),\ \ i\geq 2 \tag{2}$$

In which, $\phi_j(\xi)$ is defined in Eq.(3) as follows:

$$\phi_j(\xi)=\sqrt{\frac{2j-1}{2}}\int_{-1}^{\xi}P_{j-1}(t)dt=\frac{1}{\sqrt{2(2j-1)}}\left(P_j(\xi)-P_{j-2}(\xi)\right) \tag{3}$$

Where $P_k(\xi)$ is the Legendre polynomials:

$$P_k(\xi)=\frac{1}{2^k k!}\frac{d^k}{d\xi^k}\left(\xi^2-1\right)^k \tag{4}$$

The internal shape functions are defined for each element locally. These shape functions vanish at all the edges.

$$N_{i,j}^{\text{int}}(\xi,\eta)=\phi_i(\xi)\phi_j(\xi),\ \ i,j\geq 2 \tag{5}$$

Where the indices *i* and *j* of the shape functions denote the polynomial degrees in the local directions ξ and η, respectively. Figure 2 shows the plots of shape functions for a quadrilateral element in the trunk space [31] with $p = 1$ to $p = 8$, where polynomial degree p_ξ and p_η in directions ξ and η, respectively, are set equal to p. These shape functions are plotted according to the nodal and edge numbering convention in Figure 1.

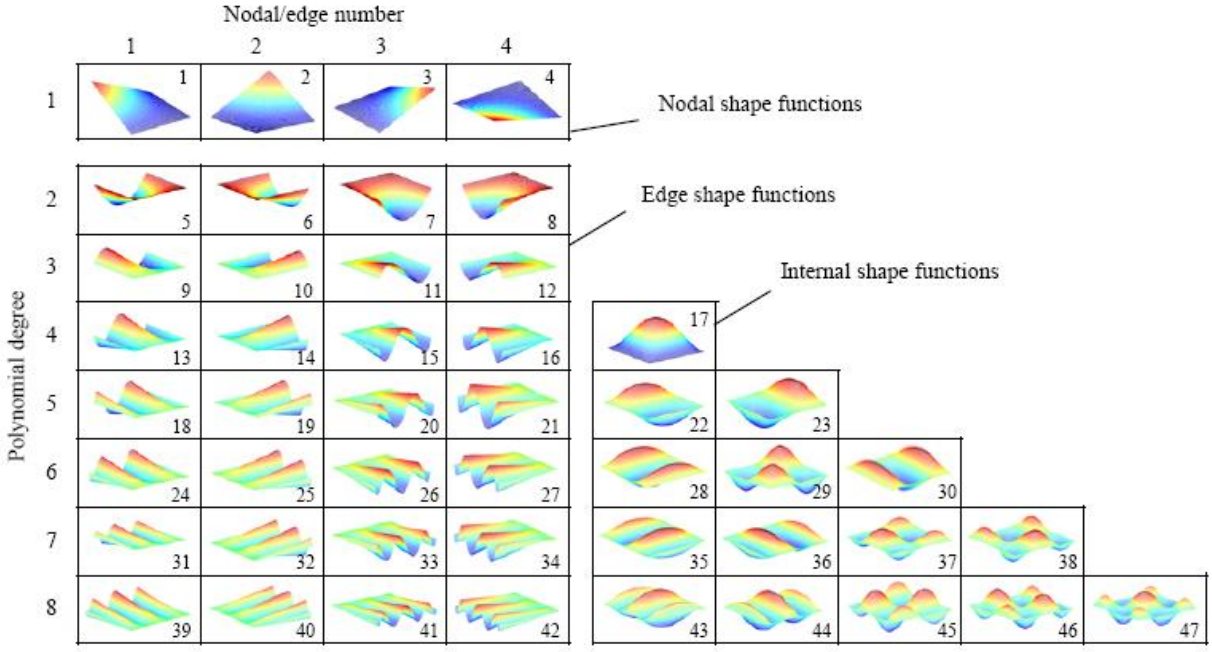

Figure 2. Hierarchical shape functions in quadrilateral element in trunk space with $p = 1$ to $p = 8$ (after [31]).

5. Multi-resolution topology optimization using the p-version finite element method

This section describes the multi-resolution topology optimization approach using the p-version FEM. The topology optimization formulation is introduced for generic minimum compliance problems.

5.1 Problem formulation

We consider the minimum compliance problem where the compliance is the objective function and the volume is the constraint.

$$\begin{aligned} \min_{\mathbf{d}} \quad & C(\rho(\mathbf{d}),\mathbf{u}) \\ s.t.: \quad & \rho = f(\mathbf{d}) \\ & \mathbf{K}(\rho(\mathbf{d}))\mathbf{u} = \mathbf{f} \\ & V(\rho(\mathbf{d})) = \int_{\Omega} \rho(\mathbf{d}) dV \le V_s \end{aligned} \tag{6}$$

Following are details of the terms used in the above equation: **u** is the vector of coefficients, which consists of the coefficients corresponding to the node, edge, face and internal shape functions. The coefficient values at the nodes equal the nodal displacement at the nodes. In this formulation, the displacement field $u_e(x)$ is interpolated using the hierarchical shape functions:

$$u_e = \mathbf{N}_e \mathbf{u}_e \tag{7}$$

Where $\mathbf{N}_e$ is the matrix of hierarchical shape functions and $\mathbf{u}_e$ is the vector of coefficients corresponding to the degrees of freedom of element *e*. The density field ρ is a function of the design variable vector **d**. The way **d** is arranged and related to the density field ρ defines the design model and will be detailed in the following section. Through using a relaxation approach, the density can have any intermediate value between 0 and 1; thus material properties are related to the intermediate density by the well-known Solid Isotropic Material with Penalization (SIMP) model [2, 27]. According to this model, the Young's modulus is computed as:

$$E(\mathbf{x}) = E_{\min} + \rho(\mathbf{x})^q (E^0 - E_{\min}) \tag{8}$$

In which E^0 is the original Young's modulus of the material in the solid phase (corresponding to the density ρ = 1), and the exponent *q* is the penalization parameter. $E_{\min}$ is a very small stiffness which is introduced to prevent singularity of the stiffness matrix. The modified SIMP model in Eq.(8) differs from the origin SIMP model in the occurrence of $E_{\min}$, therefore, a small positive lower bound on the density is not needed. When the penalization parameter *q* is greater than 1, the intermediate density approaches either 0 (void) or 1(solid).

5.2 Multi-resolution topology optimization using the p-version FEM

The design model follows the multi-resolution topology optimization (MTOP) approach, which has been successfully applied to the conventional h-version FEM in [11, 33, 34]. On top of the finite element mesh, we introduce a grid of points that represent the design variables **d** (cf. Figure 3). Each point corresponds to one design variable, which can take any value between 0 and 1. This design variable grid is independent of the finite element mesh, thus the choice the design variable and finite element discretization is flexible. The denser the design variable grid is, the higher resolution the topology optimization can be. However, increasing the number of design variables also increases the computational cost associated with the optimization. Nevertheless, the optimization computation cost is usually much smaller than that of the associated finite element analysis [4, 35].

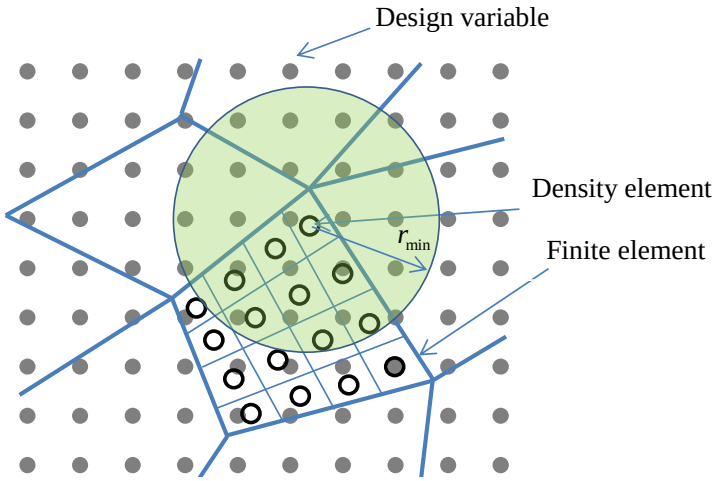

Figure 3. Design variable grid, density element, and finite element mesh

The density field inside of a finite element is computed from the design variable grid using a convolution, in this case a filter [29] as follows:

$$\rho(x) = f(\mathbf{d}) = \frac{\sum_{i \in S(x)} d_i w(r_i)}{\sum_{i \in S(x)} w(r_i)} \tag{9}$$

Where $S(x)$ is the subset of the design variable vector $\mathbf{d}$, which lies in a circle of radius $r_{\min}$ and centered at point x (cf. Figure 3). The weight $w(r_i)$ corresponding to variable d_i can be defined as follows:

$$w(r_{ni}) = \begin{cases} \dfrac{r_{\min} - r_{ni}}{r_{\min}} & \text{if } r_{ni} \le r_{\min} \\ 0 & \text{otherwise} \end{cases} \tag{10}$$

Note that the physical radius $r_{\min}$ (cf. Figure 3) is independent of the mesh. More discussion about the use of a filter in topology optimization can be found in [27-29]. In general, the filter imposes a length-scale to the resulting structure. More specifically, the size of the smallest structural member is in the range of $2r_{\min}$. The larger $r_{\min}$ is, the more restriction is imposed on the design model. The choice of the length-scale parameter $r_{\min}$ is based on two considerations. First, it has to be large enough to avoid numerical instability. The smaller $r_{\min}$ is, the higher-fidelity the design model can be. At a certain point, the analysis model is no longer accurate enough for the fidelity of the design model, and the optimization will start producing spurious results. The analysis accuracy is dependent on the polynomial degree of the p-element. For the traditional element-based approach (p = 1), the size of $r_{\min}$ must be larger than the size of the finite element. Moreover, $r_{\min}$ must be large enough such that $S(x)$ is non-empty for all points in the design space, i.e. there is no point in the design space that the filter circle does not contain any design variable. Second, designers may want to limit the complexity of a design for easier manufacturing, and produce a more well-defined result for easier interpretation. In that case, $r_{\min}$ can be determined based on the desired complexity of the design.

6. Numerical examples

To show the effectiveness of our proposed approach we solve a benchmark example, the Messerschmitt-Bolkow-Blohm (MBB beam) [33] for minimum compliance subject to volume constraint (cf. Figure 4a). The beam has a length, b = 60 and height, h = 10. To enhance convergence to global optima, the continuation technique is used on the penalization parameter q, q is initially taken as 1 and increased by 0.5 after every 30 iterations, and q is ultimately taken as 3. For this example, the analytical solution is the so-called Michell's truss [36] as shown in Figure 4b.

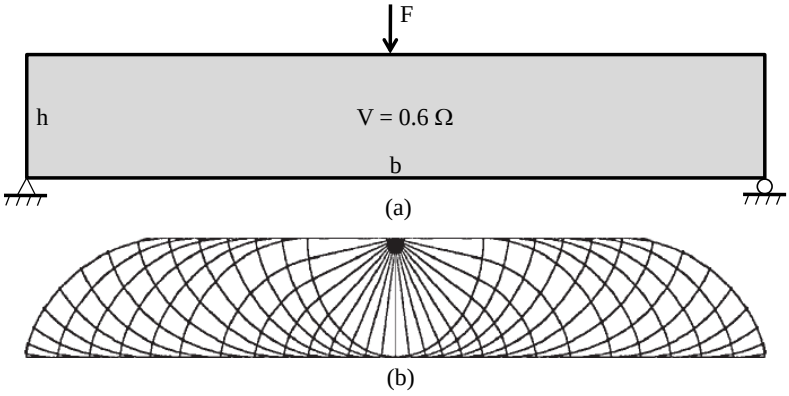

Figure 4. MBB beam example: (a) Domain, (b) Analytical solution (Michell's solution [36])

The optimization problem is first solved using the traditional element-based approach with a p-version FEM. The problem is solved for two cases, one using a density filter with a filer radius ($r_{\min}$ = 1.2), and one using no filter. In both cases, the mesh finite element mesh is 60×10. The results in Figure 5a and 5b show that increasing p from 1 to 4, and thus the number of degrees-of-freedom (DOFs) increases about 7 times, does not have significant effect on the results, indicating that the higher computational cost and higher accuracy of p-version FEM is wasted. Without the filter and for p = 2, the numerical instability is alleviated as shown in Figure 5c. However, increasing p further, p = 4, does not have significant effect on the results as shown in Figure 5d, even as the number of degrees-of-freedom (DOFs) increases by approximately a factor of 3. Note that filter introduces a gray area around structural members, otherwise the results with and without a filter have similar topology. Overall, there is no

significant improvement in the design when increasing polynomial degree p if the traditional element-based approach is employed.

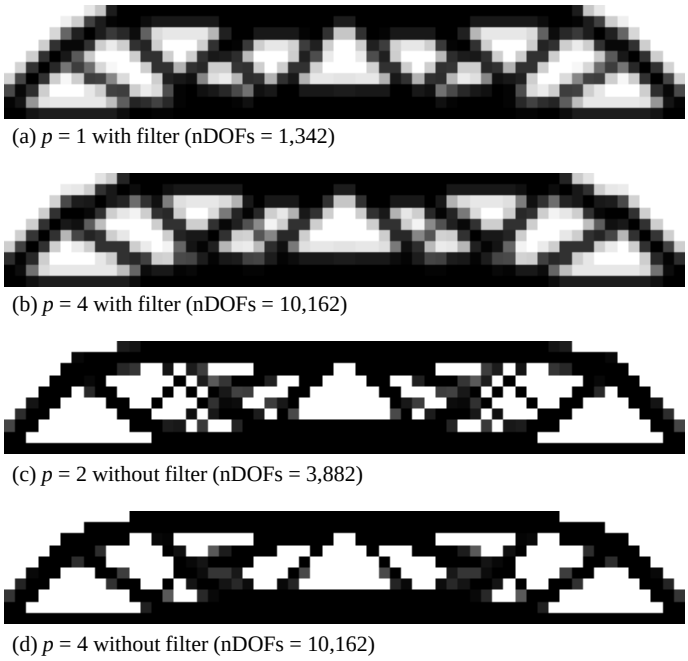

(a) p = 1 with filter (nDOFs = 1,342)

(b) p = 4 with filter (nDOFs = 10,162)

(c) p = 2 without filter (nDOFs = 3,882)

(d) p = 4 without filter (nDOFs = 10,162)

Figure 5. Problem using traditional element-based approach with p-version FEM

Next, the problem is solved using the same mesh size of 60×10, but using the proposed multi-resolution approach. Since the example uses a structured mesh, a design variable grid that is parallel to the rows and columns of the finite element mesh is chosen. The spacing of design variables is one fifth of the finite element size. For simplicity, a uniform density element mesh that has 25 density elements in each finite element is used. For each polynomial p from 1 to 6, a density filter radius that is just large enough to avoid numerical instabilities yes small enough to get as intricate structures as possible is used.

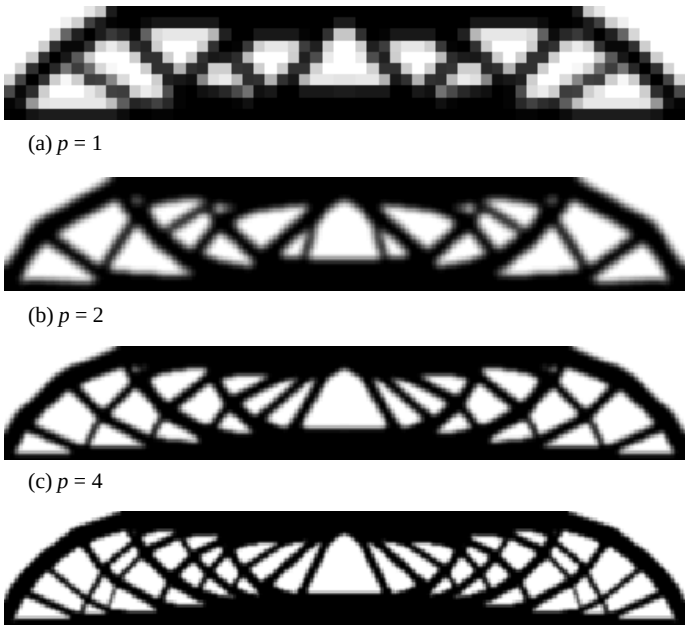

(a) p = 1

(b) p = 2

(c) p = 4

(d) p = 6

Figure 6. Results using multi-resolution approach with p-version FEM on the same mesh a (FE mesh 60×10 elements) – effect of the polynomial degree p: (a) element-based approach; (b-d) multi-resolution approach

The results in Figure 6 show that as p increases, more and more intricate structures are obtained. This increase in fidelity of the results is similar to the improvement expected with h-version FEM when the finite element mesh is refined. Note that in this case the finite element mesh stays the same, while the polynomial order increases. For comparison, the result using the traditional element-based approach is included in Figure 6a. As can be seen from Figure 6b, c, and d, the results are improved as the polynomial degree p increases. In general, increasing the p-version FEM polynomial degrees improves the intricacy of the design, which is similar to the effect of refining the finite element mesh, while increasing the number of design variables and density elements improves the resolution of the results. It is also noted that for higher p, it is possible to obtain structural members that are considerably smaller than the finite element size; this is obtained because of the increased accuracy of the p-version FEM method allows such fidelity of the design model so that smaller length-scale, i.e. filter radius, can be used to capture such fidelity. In this case, the filter radius is 1.2 for element based-approach and 0.75, 0.5 and 0.35 for p = 2, 4 and 6 for the multi-resolution approach, respectively. The results in Figure 6 show that that resolution can be improved by increasing the polynomial degree p in the p-version FEM.

7. Conclusions

Traditional element-based topology optimization has been well developed for the h-version of the finite element method. However, it does not work well with the p-version of the finite element method, which has gained popularity especially front-end analysis such as Creo and ANSYS [24, 25]. In this paper, we propose a multi-resolution topology optimization method that is more suitable for the p-version of finite element analysis. The method is based on the idea of decoupling of design model and analysis model so that the resolution for the topology description becomes flexible. This allows us to refine the design models along with the increase of polynomial order in the analysis model, even when the finite element mesh is fixed. The proposed method allows us to take full advantage of the increased analysis accuracy of the p-version FEM method for topology optimization. As the density and design variable meshes are finer than the displacement mesh, the approach enables to obtain high resolution results.

8. Acknowledgements

This research was funded in part by the National Science Foundation under the grant number CMMI 1000666 and by Northeastern University. The support is gratefully acknowledged. The opinions, findings, and conclusion stated herein are those of the authors and do not necessarily reflect those of sponsors.

9. References

[1]. M.P. Bendsøe and O. Sigmund, *Topology Optimization: Theory, Methods and Applications*, Springer, Berlin, 2004.

[2]. G. Rozvany, M. Zhou, and T. Birker, Generalized Shape Optimization without Homogenization, *Structural and Multidisciplinary Optimization*, 4(3), 250-252, 1992.

[3]. M.P. Bendsøe and O. Sigmund, Material Interpolation Schemes in Topology Optimization, *Archive of Applied Mechanics*, 69(9), 635-654, 1999.

[4]. T. Borrvall and J. Petersson, Large-Scale Topology Optimization in 3d Using Parallel Computing, *Computer Methods in Applied Mechanics and Engineering*, 190(46-47), 6201-6229, 2001.

[5]. O. Amir, M. Stolpe, and O. Sigmund, Efficient Use of Iterative Solvers in Nested Topology Optimization, *Structural and Multidisciplinary Optimization*, 42(1), 55-72, 2010.

[6]. S. Wang, E. Sturler, and G.H. Paulino, Large-Scale Topology Optimization Using Preconditioned Krylov Subspace Methods with Recycling, *International Journal for Numerical Methods in Engineering*, 69(12), 2441-2468, 2007.

[7]. O. Amir, M.P. Bendsøe, and O. Sigmund, Approximate Reanalysis in Topology Optimization, *International Journal for Numerical Methods in Engineering*, 78(12), 1474-1491, 2009.

[8]. R. Stainko, An Adaptive Multilevel Approach to the Minimal Compliance Problem in Topology Optimization, *Communications in Numerical Methods in Engineering*, 22(2), 109-118, 2006.

[9]. J.C.A. Costa Jr and M.K. Alves, Layout Optimization with H-Adaptivity of Structures, *International Journal for Numerical Methods in Engineering*, 58(1), 83-102, 2003.

[10]. S. Schmidt and V. Schulz, A 2589 Line Topology Optimization Code Written for the Graphics Card, *Computing and Visualization in Science*, 16(6), 249-256, 2012.

[11]. T.H. Nguyen, G.H. Paulino, J. Song, and C.H. Le, A Computational Paradigm for Multiresolution Topology Optimization (Mtop), *Structural and Multidisciplinary Optimization*, 41(4), 525-539, 2010.

[12]. T.H. Nguyen, J. Song, and G.H. Paulino, Single-Loop System Reliability-Based Topology Optimization Considering Statistical Dependence between Limit-States, *Structural and Multidisciplinary Optimization*, 44(5), 593-611, 2011.

[13]. T.H. Nguyen, J. Song, and G.H. Paulino, Single-Loop System Reliability-Based Design Optimization Using

Matrix-Based System Reliability Method: Theory and Applications, *Journal of Mechanical Design*, 132(1), 011005, 2010.
[14]. A. Takezawa and M. Kitamura, Geometrical Design of Thermoelectric Generators Based on Topology Optimization, *International Journal for Numerical Methods in Engineering*, 90(11), 1363-1392, 2012.
[15]. A. Sutradhar, G.H. Paulino, M.J. Miller, and T.H. Nguyen, Topological Optimization for Designing Patient-Specific Large Craniofacial Segmental Bone Replacements, *Proceedings of the National Academy of Sciences*, 107(30), 13222-13227, 2010.
[16]. N. Aage, M. Nobel-Jørgensen, C.S. Andreasen, and O. Sigmund, Interactive Topology Optimization on Hand-Held Devices, *Structural and Multidisciplinary Optimization*, 47(1), 1-6, 2013.
[17]. S.L. Vatanabe, G.H. Paulino, and E.C.N. Silva, Influence of Pattern Gradation on the Design of Piezocomposite Energy Harvesting Devices Using Topology Optimization, *Composites Part B: Engineering*, 43(6), 2646-2654, 2012.
[18]. Z. Luo, N. Zhang, W. Gao, and H. Ma, Structural Shape and Topology Optimization Using a Meshless Galerkin Level Set Method, *International Journal for Numerical Methods in Engineering*, 90(3), 369-389, 2012.
[19]. J. Zhou and W. Zou, Meshless Approximation Combined with Implicit Topology Description for Optimization of Continua, *Structural and Multidisciplinary Optimization*, 36(4), 347-353, 2008.
[20]. K. Abe, S. Kazama, and K. Koro, A Boundary Element Approach for Topology Optimization Problem Using the Level Set Method, *Communications in Numerical Methods in Engineering*, 23(5), 405-416, 2007.
[21]. A. Canelas, J. Herskovits, and J. Telles, Shape Optimization Using the Boundary Element Method and a SAND Interior Point Algorithm for Constrained Optimization, *Computers & Structures*, 86(13), 1517-1526, 2008.
[22]. A. Gersborg-Hansen, M.P. Bendsøe, and O. Sigmund, Topology Optimization of Heat Conduction Problems Using the Finite Volume Method, *Structural and Multidisciplinary Optimization*, 31(4), 251-259, 2006.
[23]. L. Dedè, M.J. Borden, and T.J.R. Hughes, Isogeometric Analysis for Topology Optimization with a Phase Field Model, *Archives of Computational Methods in Engineering*, 19(3), 427-465, 2012.
[24]. R. Toogood and J. Zecher, *Creo Parametric 2.0 Tutorial*, SDC Publications, 2013.
[25]. A. Release, 10.0, *Documentation for ANSYS*, 2005.
[26]. A. Diaz and O. Sigmund, Checkerboard Patterns in Layout Optimization, *Structural and Multidisciplinary Optimization*, 10(1), 40-45, 1995.
[27]. O. Sigmund, Morphology-Based Black and White Filters for Topology Optimization, *Structural and Multidisciplinary Optimization*, 33(4), 401-424, 2007.
[28]. J. Guest, J. Prévost, and T. Belytschko, Achieving Minimum Length Scale in Topology Optimization Using Nodal Design Variables and Projection Functions, *International Journal for Numerical Methods in Engineering*, 61(2), 238-254, 2004.
[29]. T.E. Bruns and D.A. Tortorelli, Topology Optimization of Non-Linear Elastic Structures and Compliant Mechanisms, *Computer Methods in Applied Mechanics and Engineering*, 190(26-27), 3443-3459, 2001.
[30]. J. Parvizian, A. Düster, and E. Rank, Topology Optimization Using the Finite Cell Method, *Optimization and Engineering*, 13(1), 57-78, 2012.
[31]. B.A. Szabo and I. Babuska, *Finite Element Analysis*, Wiley New York, 1991.
[32]. R.D. Cook, *Concepts and Applications of Finite Element Analysis*, John Wiley & Sons, 2007.
[33]. T.H. Nguyen, G.H. Paulino, J. Song, and C.H. Le, Improving Multiresolution Topology Optimization Via Multiple Discretizations, *International Journal for Numerical Methods in Engineering*, 92(6), 507-530, 2012.
[34]. T.H. Nguyen, *System Reliability-Based Design and Multiresolution Topology Optimization*, Ph.D thesis, *Department of Civil and Environmental Engineering*, University of Illinois at Urbana-Champaign, Urbana, 2010.
[35]. S. Wang, E. de Sturler, and G.H. Paulino, Large-Scale Topology Optimization Using Preconditioned Krylov Subspace Methods with Recycling, *International Journal for Numerical Methods in Engineering*, 69(12), 2441-2468, 2007.
[36]. G. Rozvany, Some Shortcomings in Michell's Truss Theory, *Structural and Multidisciplinary Optimization*, 12(4), 244-250, 1996.